Tropomyosin regulates cell migration during skin wound healing.

Justin G. Lees[1], Yu Wooi Ching[1], Damian Adams[2], Cuc T.T. Bach[1], Michael S. Samuel[4], Anthony Kee[5], Edna Hardeman[5], Peter Gunning[6], Allison Cowin[2] and Geraldine M. O'Neill[1,3]*

[1]Children's Cancer Research Unit, Kids Research Institute, The Children's Hospital at Westmead, Westmead, New South Wales, 2145, Australia, [2]Women's and Children's Health Research Institute, South Australia, 5006, Australia, [3]Discipline of Paediatrics and Child Health, The University of Sydney, Sydney, New South Wales, 2006, Australia, [4]Centre for Cancer Biology, SA Pathology & The University of Adelaide, South Australia, 5000, Australia, [5]Neuromuscular and Regenerative Medicine Unit, School of Medical Sciences, The University of New South Wales, NSW 2052, Australia and [6]Oncology Research Unit, School of Medical Sciences, The University of New South Wales, NSW 2052, Australia.

Work was completed in Sydney, NSW, Australia.

*Corresponding Author:
Geraldine M. O'Neill
Children's Cancer Research Unit
The Children's Hospital at Westmead
Locked Bag 4001, Westmead, 2145
Australia
Ph: 61 2 98451206
Fax: 61 2 98453078
Email: geraldine.oneill@health.nsw.gov.au

Running title: Wound healing is accelerated in Tm5NM1/2 knockout mice.

Abbreviations: Wildtype (WT), Unwounded (UW), tropomyosin 5 non-muscle 1 (Tm5NM1)

Abstract

Precise orchestration of actin polymer into filaments with distinct characteristics of stability, bundling and branching underpins cell migration. A key regulator of actin filament specialization is the tropomyosin family of actin-associating proteins. This multi-isoform family of proteins assemble into polymers that lie in the major groove of polymerized actin filaments, which in turn determine the association of molecules that control actin filament organization. This suggests that tropomyosins may be important regulators of actin function during physiological processes dependent on cell migration such as wound healing. We have therefore analysed the requirement for tropomyosin isoform expression in a mouse model of cutaneous wound healing. We find that mice, in which the 9D exon from the TPM3/γTm tropomyosin gene is deleted (γ9D -/-), exhibit a more rapid wound healing response 7 days after wounding compared to Wildtype (WT) mice. Accelerated wound healing was not associated with increased cell proliferation, matrix remodelling or epidermal abnormalities but with increased cell migration. Rac GTPase activity and paxillin phosphorylation are elevated in cells from γ9D -/- mice, suggesting activation of paxillin/Rac signalling. Collectively, our data reveal that tropomyosin isoform expression plays an important role in temporal regulation of cell migration during wound healing.

Introduction

Wound healing is an orchestrated multi-tissue response, requiring cell migration (Singer and Clark, 1999). Different phases of wound healing follow an orderly timetable, with each phase preparing the wound for subsequent steps necessary to restore the tissue barrier. An important step in this timetable is the migration of keratinocytes and fibroblasts into the wound bed. Approximately 7 days after wounding, fibroblasts move into the wounded area along collagen fibres and recruitment of these cells to the wound subsequently regulates matrix reorganization and wound contraction (Clark *et al.*, 2007; Gurtner *et al.*, 2008; Tomasek *et al.*, 2002). Central to the ability of fibroblasts and keratinocytes to move into the wound area is a dynamic and responsive actin cytoskeleton. Emphasizing the requirement for an orderly execution of the wound healing timetable, manipulations that increase the rate of dermal fibroblast infiltration correspondingly cause more rapid wound closure (Reynolds *et al.*, 2005). Thus molecules which regulate actin filament dynamics and thereby change the rate of cell migration can alter the rate of wound healing (Castilho *et al.*, 2010; Cowin *et al.*, 2007; Kopecki and Cowin, 2008; Liu *et al.*, 2009; Tscharntke *et al.*, 2007; Witke *et al.*, 1995). The tropomyosin family of actin-associating proteins display tissue-specific and time-dependent expression and their association with actin filaments imparts isoform-specific regulation of the associated actin filament (Gunning *et al.*, 2008). While there is mounting in vitro evidence that tropomyosins regulate cell migration (Lees *et al.*, 2011a), the role of these proteins has not previously been examined during in vivo wound healing.

Tropomyosins assemble as polymers that lie in the major groove of polymerized actin filaments (Gunning *et al.*, 2008). Tropomyosin association with actin filaments in turn determines the association of molecules that control actin filament turnover (Blanchoin *et al.*, 2001; Bryce *et al.*, 2003; Ishikawa *et al.*, 1989). Thus the pattern of tropomyosin decoration of actin filaments defines the function of the associated filament (Gunning *et al.*, 2008). Low-molecular weight non-muscle tropomyosin isoforms Tm5NM1 and Tm5NM2 are two splice forms from the TPM3/γTm gene containing exon 9D from this gene sequence. We have previously shown that elevated Tm5NM1 expression inhibits cell migration in vitro and inversely correlates with the rate of elongated, adhesion-dependent cell migration in 3-dimensional collagen gels (Bach *et al.*, 2009; Lees *et al.*, 2011b). Significantly, elongated, adhesion-dependent migration is used by fibroblasts and keratinocytes during wound healing.

The elongated form of cell migration exhibited by fibroblasts relies on activation of the small GTPase Rac (Sanz-Moreno *et al.*, 2008), which stimulates formation of lamellipodia and small precursor adhesion complexes at the leading edge (Nobes and Hall, 1995). In vivo, conditional Rac1 deletion in epidermal keratinocytes (Castilho *et al.*, 2010; Tscharntke *et al.*, 2007) and dermal fibroblasts (Liu *et al.*, 2009) significantly impairs wound healing. Studies in vitro have revealed that Rac activity is required in fibroblasts for lamellipodial persistence and migration in scratch wound healing assays (Nobes and Hall, 1999). Our previous work showing that fibroblasts derived from mice lacking Tm5NM1/2 have increased Rac-dependent formation of precursor adhesions and strikingly increased persistence when migrating into a scratch wound in vitro (Bach *et al.*,

2009) thus suggests that Rac activity may be increased in these mice, potentially leading to accelerated wound healing.

Adhesion proteins such as paxillin that are phosphorylated by Src kinase are major regulators of Rac GTPase activity at the leading edge. Upon phosphorylation by Src, paxillin recruits Rac guanine nucleotide exchange factor DOCK180 to the leading edge by binding to the adaptor protein Crk, which is constitutively associated with DOCK180 (Valles *et al.*, 2004). DOCK180 in turn catalyzes Rac activation (Kiyokawa *et al.*, 1998). Critical to this process is disassembly of mature focal adhesions at the base of the lamellipodium, which are associated with bundles of polymerized actin in the cell body. The disassembly of these sites precedes the formation of new Rac-dependent adhesions at the leading edge of the cell (Webb *et al.*, 2003) and increased tension on the actin filament is suggested to reduce phosphorylation of paxillin at focal adhesion sites (Zaidel-Bar *et al.*, 2007). Elevated Tm5NM1 expression inhibits Src activation (Lees *et al.*, 2011b), stabilizes mature focal adhesions (Bach *et al.*, 2009), increases myosin II recruitment and actin filament tension (Bryce *et al.*, 2003) and is inversely correlated with phosphorylation of paxillin (Bach *et al.*, 2009). Conversely genetic deletion of Tm5NM1 leads to increased Rac-dependent pre-cursor adhesion and lamellipodial formation (Bach *et al.*, 2009).

The levels of Tm5NM1/2 in different organs in the body range from low levels in the heart and muscle to many-fold increased levels in organs such brain, kidney and spleen (Schevzov *et al.*, 2011). The function of these isoforms in the skin and how changes in

their expression might regulate the wound healing response requires further investigation. We therefore sought to understand the role of tropomyosin in the process of full thickness skin wound healing in Tm5NM1/2 homozygous knockout mice and Tm5NM1 overexpressing transgenic mice. We show that wound healing is accelerated in Tm5NM1/2 -/- mice and that this may be due to effects on a paxillin/Rac migration signalling axis.

Results

Wound healing is accelerated in Tm5NM1/2 knockout mice.

We investigated the role of tropomyosins in regulating actin filament function during cell migration in vivo using a mouse model in which both copies of the TPM3/γTm gene exon 9D are deleted (γ9D -/-), resulting in the loss of two tropomyosin isoforms, Tm5NM1 and Tm5NM2 (Fig 1a) (Fath *et al.*, 2010). Measurement of cutaneous wound healing response revealed that at 7 days after wounding, Tm5NM1/2 -/- mice exhibited significantly shorter wound lengths than similarly treated WT control mice (Fig 1b, c). The acceleration in wound healing was restricted to the 7 day time point as at all other time points analysed (3, 14 and 21 days) there was no significance difference in the distance between the epithelial layers at the wound edge (Fig 1c). Comparison of total wound area and wound gape confirmed that at day 7 the wound area and gape was significantly smaller in the Tm5NM1/2 -/- mice (Fig 1d, e, f). Collectively, these measurements reveal that wound healing is specifically increased at day 7 in the mice lacking Tm5NM1/2.

We next examined whether Tm5NM1/2 depletion altered skin tissue organization. Histological examination revealed no obvious differences in the structure of the epidermis, dermis, panniculus muscle and adipose tissue (Fig 1b and Fig 2a). Moreover, analysis of the epidermal layer by E-cadherin staining similarly revealed comparable organization in Tm5NM1/2 -/- and WT mice (Fig 2a). To determine whether Tm5NM1/2 depletion might alter the distribution of collagen fibres critical to the wound healing response, we used picrosirius red (PSR) staining to measure collagen fibre distribution

(Fig 2b). This revealed no difference in collagen fibre distribution between WT and Tm5NM1/2 -/- mice, either in unwounded (UW) skin or after wounding (Fig 2b, c). Since cell proliferation plays a critical role in the wound healing response, we investigated whether increased proliferation could explain the accelerated wound healing in Tm5NM1/2 -/- mice. PCNA staining in the wound dermal region revealed no significant difference in the numbers of proliferating cells in WT and Tm5NM1/2 -/- mice (Fig 2d). Similarly, quantification of proliferating epidermal cells at day 3 after wounding revealed no significant differences. Using a collagen gel contraction assay we confirmed that increased wound healing is not due to increased contractility as the Tm5NM1/2 -/- MEFs did not display altered gel contraction (Figure 2e). Furthermore, there was no significant difference in the gape measured between the edges of the panniculus carnosus on either side of the wound at any time point regardless of genotype (Figure 2f). Collectively these analyses suggest that accelerated wound healing in the Tm5NM1/2 -/- mice is not due to altered structure of skin tissue, changes in cell proliferation or increased contractility.

As fibroblasts and keratinocytes are the two major motile cell populations that mediate wound closure in the skin we determined whether these cells express Tm5NM1/2. Non-specific antibody cross-reaction prevented analysis of Tm5NM1/2 by immunohistochemistry in tissue sections. Expression was therefore instead analysed in lysates extracted from isolated populations of primary fibroblasts and keratinocytes. This confirmed that both of these important motile cell types express endogenous Tm5NM1/2, at approximately equal levels (Fig 3a, b). We next analysed endogenous Tm5NM1/2 expression in protein extracts of skin tissue at different time points after wounding in WT

mice. This revealed a striking up-regulation of Tm5NM1/2 expression in response to wounding (Fig 3c, d). Tm5NM1 levels were significantly increased at day 3 after wounding and gradually decreased over time (Fig 3c, d) suggesting either increased expression in cells present in the wound or the migration of Tm5NM1/2 positive cells into the wound area. Thus, we next examined whether elevated Tm5NM1 expression alters wound healing by employing a transgenic mouse that expresses human Tm5NM1 (+/WT). Expression of the exogenous human transgene was confirmed by probing with LC1 antibody that specifically binds human Tm5NM1/2 (Schevzov *et al.*, 2005) (Fig 3e). Increased total Tm5NM1 expression was confirmed by analysis with anti-γ9D antibodies that bind both endogenous mouse and exogenous human protein (Figure 3f and g). Analysis of the wound healing response in the transgenic mice revealed no significant difference in the wound lengths at either day 3 or day 7 after wounding between the WT and the transgenic overexpressing mice (Fig 3h). Thus, exogenous Tm5NM1 expression does not appear to alter cutaneous wound healing. Notably, increased Tm5NM1 expression observed at day 3 in the wild-type mice (Fig 3c, d) is also observed in the transgenic mice (Fig 3 i, j).

Tm5NM1/2 deletion activates a paxillin/Rac signalling axis

Our previous work has suggested that Tm5NM1 expression is inversely correlated with activation of Src kinase and its down-stream substrate paxillin (Bach *et al.*, 2009; Lees *et al.*, 2011b). Since the phosphorylation of paxillin by Src kinase stimulates cell migration (Zaidel-Bar *et al.*, 2007), we analysed paxillin expression and phosphorylation in UW skin. There was a trend for increased paxillin expression in UW skin from knock-out

mice (Figure 4a) and total paxillin phosphorylation was significantly increased (Figure 4a). Paxillin is reported to signal down-stream to induce the activation of Rac GTPase (Valles *et al.*, 2004) and we have previously shown that embryonic fibroblasts from Tm5NM1/2 -/- mice exhibit increased Rac-dependent formation of focal complexes and lamellipodia (Bach *et al.*, 2009). Therefore, we hypothesized that Rac activation may underlie the increased migration in cells lacking Tm5NM1/2. Analysis of total Rac protein levels revealed that Rac expression was significantly increased in Tm5NM1/2 -/- cells compared to WT cells (Fig 4b). We then quantified Rac activity via GST pull-down assays and observed that Rac activity was also significantly increased in Tm5NM1/2 -/- cells (Fig 4c). We next addressed whether the increase in Rac activity could be attributed specifically to deletion of the Tm5NM1 isoform, as our previous work has established that high levels of Tm5NM1 can suppress cell migration (Bach *et al.*, 2009; Bryce *et al.*, 2003; Lees *et al.*, 2011b). This was addressed by analysing Rac expression and activity in a cell line that was created to express high level exogenous Tm5NM1 (Bryce *et al.*, 2003). Importantly, both total Rac protein and Rac GTPase activity are significantly reduced in cells with high level levels of Tm5NM1 (Fig 4b,c).

As Rac activity stimulates the formation of lamellipodia, we examined sub-cellular distribution of Tm5NM1 during lamellipodial extension. Tm5NM1/2 -/- mouse embryo fibroblasts were transfected with YFP-tagged Tm5NM1 and observed by time-lapse imaging. Fluorescently-tagged Tm5NM1 was incorporated into actin stress fibres that traverse the cell body (Fig 5a). At the leading edge, the lamellipodium extends beyond the ends of Tm5NM1-positive filaments and the newly extended membrane is free of

Tm5NM1-positive filaments (arrow heads, Fig 5a). Subsequently, Tm5NM1-positive filaments formed in the lamellipodium and along the edge of the protruded membrane (arrows, Fig 5a). Tm5NM1-positive filaments at the membrane edge and in the lamellipodium then were frequently observed to join together with Tm5NM1 positive filaments in the cell body (Supplementary movie 1). We have previously demonstrated increased lamellipodial formation in Tm5NM1/2-/- MEFs by scoring for the presence of paxillin-positive focal complexes (Bach *et al.*, 2009). Importantly, we here show that exogenous Tm5NM1 expression reduces lamellipodia formation in the Tm5NM1/2-/- MEFs (Fig 5b and c). Rescue experiments with exogenous Tm5NM2 that also localizes to stress fibres in the Tm5NM1/2-/- MEFs (Fig 5b), similarly reduced lamellipodial formation (Fig 5c). Thus restoration of exon 9D-containing products can inhibit the increased lamellipodial formation that occurs in the absence of these isoforms.

Discussion

Mounting research has pointed to an important role for tropomyosins in specialising actin filament function, to coordinate the morphologies and force that underpin cell migration (Lees *et al.*, 2011a). In the present study, we have investigated the role of γ9D exon-containing isoforms from the γTm/*TPM3* tropomyosin gene. Our studies reveal a change in the timing of wound healing in the absence of these gene products. We further show in cultured cells that elevated Tm5NM1 isoform expression causes the opposite effects to those seen in Tm5NM1/2 -/- fibroblasts. Together with recent studies showing that the drosophila tropomyosin *TM1* gene is required for drosophila oocyte border cell migration (Kim *et al.*, 2011), it appears that tropomyosins indeed have a role during physiological cell migration.

In Tm5NM1/2 -/- mice, wound healing was specifically increased 7 days after wounding, while at later time points there was no difference in the wound size between the WT and knockout mice. Similarly, heterozygous deletion of FliI, homozygous deletion of glycogen synthase kinase-3 (GSK-3) and targeted homozygous deletion of the α3 integrin subunit in the basal layer of the epidermis, all lead to smaller wound areas ~ 7 days after wounding (Cowin *et al.*, 2007; Kapoor *et al.*, 2008; Margadant *et al.*, 2008). While each of these genetic approaches promoted increased migration responses in isolated skin cells, they differ in the effects on proliferation and collagen deposition in the wound bed. Our results suggest that there is no change in proliferation, collagen composition or contractility in the Tm5NM1/2 -/- mice. Notably, while the effects of GSK-3 deletion persisted throughout the time course of wound healing (Kapoor *et al*,.

2008), similar to our findings, FliI effected the extent of wound healing at 7 days but by day 14 there was no difference between the controls and mice with genetically altered FliI expression (Cowin *et al*., 2007). Given the temporal separation of different phases of wound healing, our findings and the earlier data with FliI suggest that actin regulators may play a specific role during the migration phase that occurs at around 7 days after wounding.

We have previously shown that re-expression of exogenous Tm5NM1 reduces the migration speed of Tm5NM1/2 -/- mouse embryo fibroblasts (Bach *et al.*, 2009). Together with the observation that Tm5NM1/2 -/- mice exhibit more rapid wound healing, we thus hypothesized that transgenic overexpression of Tm5NM1 might cause delayed wound healing. However, there was no significant difference in wound healing between WT and transgenic mice expressing the human Tm5NM1 gene. We note that the inhibition of cell migration by Tm5NM1 requires high level exogenous Tm5NM1 expression (Bach *et al.*, 2009; Bryce *et al.*, 2003). Potentially therefore the levels of Tm5NM1 expression in the transgenic mice were not sufficient to inhibit migration in the wound bed. However, we observed no correlation between the levels of exogenous Tm5NM1 expression and wound size (data not shown). Thus we suggest that it may be more likely, since endogenous Tm5NM1/2 is up-regulated following wounding, that there is a threshold effect of Tm5NM1 on wound healing such that the increase in total Tm5NM1 levels in the transgenic mice has no additional effect above that seen with endogenous Tm5NM1/2. Birth of γ9D -/- mice at less than expected Mendelian frequency (Hook *et al.*, 2011) suggests that these forms are required for efficient embryogenesis.

Given the extensive migration events that occur during embryogenesis, potentially Tm5NM1/2 is required for specific migration events during embryogenesis, such as have been reported in drosophila embryos (Kim *et al.*, 2011).

Previous work has established that Rac is a major regulator of the rate of wound healing. Mice expressing dominant negative Rac in the skin keratinocytes show delayed wound healing (Tscharntke *et al.*, 2007) and conditional deletion of Rac from either epithelial cells or fibroblasts resulted in significantly delayed wound healing (Castilho *et al.*, 2010; Liu *et al.*, 2009). Thus it is significant that both Rac protein and activity are significantly increased in Tm5NM1/2 -/- mouse embryo fibroblasts. Moreover, we show that in cells with elevated levels of Tm5NM1 expression Rac activity and protein expression is, conversely, significantly reduced. Given that Tm5NM1/2 is up-regulated subsequent to wound healing, we suggest that this may be part of a mechanism to regulate Rac activation and thus ensure that cell migration occurs in a timely fashion. Since Src phosphorylation of paxillin subsequently leads to Rac activation, increased expression of phosphorylated paxillin in Tm5NM1/2 -/- mice suggests hyper-activation of a paxillin/Rac signalling axis in the wounds of these mice. The spatial and temporal distribution of Tm5NM1 during lamellipodial extension suggests that the formation of Tm5NM1-decorated actin filaments correlates with local down-regulation of Rac activity. Moreover, extension of lamellipodia and formation of paxillin-positive focal complexes are Rac-dependent events and we show that exogenous expression of either Tm5NM1 or Tm5NM2 can suppress focal complex/lamellipodial formation in the Tm5NM1/2-/- MEFs. Our observation that Rac activity is inversely correlated with the expression of

Tm5NM1 suggests that Tm5NM1 may play a direct role in determining localized Rac activation.

An important question raised by our study is how an actin associating molecule such as Tm5NM1 might regulate Rac expression and activity. It was recently demonstrated that depletion of the αTM/*TPM1* gene products promotes Smurf1-mediated degradation of RhoA GTPase (Wong *et al.*, 2011). In contrast, depleting βTM/*TPM2* gene products had no effect on RhoA GTPase protein levels. Moreover, exogenous expression of isoform Tm2 from the αTM/*TPM1* gene competed with Smurf1 for binding to RhoA, leading to RhoA protein stabilization. It is possible that Tm5NM1/2 may similarly regulate Rac GTPase protein expression. Alternatively, increased levels of phosphorylated paxillin and Rac GTPase activity in the Tm5NM1/2 -/- mouse embryo fibroblasts may represent a change in the mechanotransduction of these cells. Paxillin at focal adhesions is reported to undergo de-phosphorylation in response to increased tension through the associated actin filament (Zaidel-Bar *et al.*, 2007). Since Tm5NM1 concentrates at the distal ends of stress fibres associated with focal adhesions (Tojkander *et al.*, 2011) it localizes to the right location to have an effect on tension-dependent dephosphorylation of paxillin. Thus, when Tm5NM1 is present it may mediate tension-dependent dephosphorylation of paxillin, leading to locally decreased Rac GTPase activation. Conversely, in the absence of Tm5NM1 this control is lost leading to increased paxillin phosphorylation and increased Rac GTPase activity.

Materials and Methods

Cell culture, antibodies and expression constructs

Tm5NM1/2 homozygous null (-/-) and wild-type mouse embryo fibroblasts (MEF) and B35 rat neuroblastoma cells over-expressing exogenous human Tm5NM1 and conditions for transfection have been previously described (Bach *et al.*, 2009). Keratinocytes extracted from the tail skin of WT mice have been described previously (Samuel *et al.*, 2011). Primary antibodies include: E-cadherin (1:250, Abcam, Cambridge, UK); proliferating cell nuclear antigen (PCNA) (1:200, Santa Cruz, CA), sheep anti-γ9D (1:500) (Schevzov *et al.*, 2011) recognising Tm5NM1/2; mouse anti-human Tm5NM1/2 (1:200) (LC1 clone); paxillin (1:500, BD bioscience, Franklin Lakes, NJ); phosphorylated paxillin (1:500, Invitrogen, Carlsbad, CA); anti-Rac (1:500, Cell Biolabs, San Diego, CA), HSP70 and HSP90 (Sigma, St Louis, MO); and GAPDH (Invitrogen, Carlsbad, CA). HRP-conjugated secondary antibodies for western blot were from Jackson Laboratories (Bar Harbor, ME), fluorescently tagged secondary antibodies for immunofluorescence from Invitrogen (Carlsbad, CA) and biotinylated horse anti-mouse IgG for immunohistochemistry from Vector Laboratories (Burlingame, CA).

Cutaneous wound healing

Mouse experiments were approved and performed in accordance with the Adelaide Women's and Children's Hospital Animal Care and Ethics Committee guidelines or the Australian National University Animal Ethics Committee following the Australian Code of Practice for the Care and the Use of Animals for Scientific Purposes. Tm5NM1/2 deficient homozygous null mice (γ9D -/-) and transgenic animals expressing exogenous

human Tm5NM1 have been previously described (Schevzov *et al.*, 2008; Vlahovich *et al.*, 2009; Bryce *et al.*, 2003), except that in the present study the Tm5NM1 transgene was transferred to the C57BL/6JArc mouse strain using speed congenic breeding. Both the Tm5NM1/2 null and Tm5NM1 transgenic mice were bred onto the C57BL/6JArc background for >10 generations. Two full-thickness 1 cm incisions were created on the dorsal skin of female, age matched (12-14 week) mice using the protocol previously described (Kopecki *et al.*, 2007). Wound gape representing the average distance between opposing edges of the wound and wound area representing the total area visibly wounded were analysed with Image-Pro Plus 5.1 (Media Cybernetics Inc, Bethesda, MD). Wound length and panniculus gape were quantified by two separate, blinded investigators by measuring distance along the wound contour between the epithelium and between panniculus edges on either side of the wound from haematoxylin–eosin (H&E) stained 4μm sections.

Histology and immunohistochemistry

Tissue sections were blocked (PBS/1% donkey serum/1% fatty acid free BSA for E-cadherin; PBS/3% normal horse serum for PCNA) then incubated with primary and secondary antibodies in the same blocking buffer. PCNA-stained sections were developed using Vectastain ABC Kit followed by DAB kit (Vector Laboratories, Burlingame, CA) then dehydrated and mounted. Sections for immunofluorescence were mounted with Prolong gold containing DAPI (Invitrogen, Carlsbad, CA). Fluorescently stained sections were imaged under an Olympus IX81 inverted microscope, with a 20X Air objective, NA0.45, using an ORCA ERG cooled CCD camera (Hamamatsu/SDR Clinical

Technology, Hamamatsu City, Japan) and bright-field imaging of tissue sections was performed using an Aperio Scanscope with a 20 Air objective (Aperio, Vista, CA, USA). Picrosirius Red (PSR) staining of paraffin embedded mice tissue sections (5μm) was performed by the ICPMR, Westmead hospital and sections imaged using a Leica DC 500 microscope with simplified polarized microscopy capability. Collagen fibre analyses were performed using Metamorph V7.0 colour separate function. Using only the hue component and a histogram of hue frequency from the resolved 8-bit images containing 256 colours, hue definitions representing different collagen fibre thickness were quantified accordingly: red 2-9 and 230-256 (thickest fibres), orange 10-38 (thick fibres), yellow 39-51 (thin fibres), green 52-128 (thinnest fibres) (Rich and Whittaker, 2005). Dermal proliferation was scored by counting PCNA positive nuclei in a defined area of the dermal bed, in four fields of view from three independent mice. Epidermal proliferation was scored by counting the percentage of PCNA positive nuclei touching the basement membrane, within 1mm from the edge of the migrating tongue, in three independent mice for each treatment condition. Image analysis was performed using Metamorph V7.0 (Leica, Solms, Germany) and final micrograph images were prepared using Photoshop C2S (Adobe, San Jose, CA).

Protein extraction and immunoblotting

Wound tissue samples were diced with surgical scissors, then lysed on ice using vigorous dissociation through a 19 gauge needle in 0.1% RIPA-SDS buffer (50mM Tris [pH7.4], 150mM NaCl, 5mM EDTA, 1% Nonidet P-40, 1% Na. Deoxycholate, 0.1% SDS freshly supplemented with 1 mM phenylmethylsulfonyl fluoride, 0.01 mg/ml aprotinin, 0.01

mg/ml leupeptin, and 1 mM Na_3VO_4). Cultured cells were lysed on ice in PTY buffer containing protease inhibitors (Cowell *et al.,* 2006). Protein concentrations were determined using the BCA Protein Assay Kit (Pierce Biotechnology, Rockford, IL) and equalized prior to SDS-PAGE. Conditions of immunoblotting were performed as previously described (Cowell *et al.*, 2006).

Rac activity assay, lamellipodia analysis and collagen gel contraction

Isolation and quantification of active Rac GTPase was performed by GST pull down as per the manufacturer's instructions (Cell Biolabs, San Diego, CA). Results were quantified by densitometry. Paxillin immunofluorescence and assessment of focal complex positive lamellipodia were performed as previously described (Bach *et al.,* 2009). For collagen gel contraction 2.5 x 10^5 WT or Tm5NM1 -/- MEF were seeded in 500µl of 2.5mg/ml rat tail collagen gels (BD bioscience) in 24 well plates. After 48 hours gels were released and contraction was quantified by measuring gel area after 3 days (Metamorph V7.0)

Statistical analysis

All error bars on histograms represent the standard error mean (S.E.M.). Statistical comparison of two means was performed by using Student's *t*-test (GraphPad, La Jolla, CA) and comparison of more than two means was performed using one-way Analysis Of Variance with Tukey's Multiple Comparison Test.

Conflict of interest

The authors declare no conflict of interest.

Acknowledgements

This study was supported by National Health and Medical Research Council (NHMRC) grant 512251 (GO and PG) and a Ramaciotti Establishment grant and Australian Society for Medical Research domestic travel award to JL. CB is the recipient of an NHMRC post-graduate scholarship and a NSW Cancer Institute Scholar award. The authors are grateful for the support of the Kid's Cancer Project. CB and AK are C4 Fellows of the Kid's Cancer Project.

References:

Bach CT, Creed S, Zhong J, Mahmassani M, Schevzov G, Stehn J, *et al.* (2009) Tropomyosin isoform expression regulates the transition of adhesions to determine cell speed and direction. *Mol Cell Biol* 29:1506-14.

Blanchoin L, Pollard TD, Hitchcock-DeGregori SE (2001) Inhibition of the Arp2/3 complex-nucleated actin polymerization and branch formation by tropomyosin. *Curr Biol* 11:1300-4.

Bryce NS, Schevzov G, Ferguson V, Percival JM, Lin JJ, Matsumura F, *et al.* (2003) Specification of actin filament function and molecular composition by tropomyosin isoforms. *Mol Biol Cell* 14:1002-16.

Castilho RM, Squarize CH, Leelahavanichkul K, Zheng Y, Bugge T, Gutkind JS (2010) Rac1 is required for epithelial stem cell function during dermal and oral mucosal wound healing but not for tissue homeostasis in mice. *PloS one* 5:e10503.

Clark RA, Ghosh K, Tonnesen MG (2007) Tissue engineering for cutaneous wounds. *J Invest Dermatol* 127:1018-29.

Cowell LN, Graham JD, Bouton AH, Clarke CL, O'Neill GM (2006) Tamoxifen treatment promotes phosphorylation of the adhesion molecules, p130Cas/BCAR1, FAK and Src, via an adhesion-dependent pathway. *Oncogene* 25:7597-607.

Cowin AJ, Adams DH, Strudwick XL, Chan H, Hooper JA, Sander GR, *et al.* (2007) Flightless I deficiency enhances wound repair by increasing cell migration and proliferation. *J Pathol* 211:572-81.

Fath T, Agnes Chan YK, Vrhovski B, Clarke H, Curthoys N, Hook J, *et al.* (2010) New aspects of tropomyosin-regulated neuritogenesis revealed by the deletion of Tm5NM1 and 2. *Eur J Cell Biol* 89:489-98.

Gunning P, O'Neill G, Hardeman E (2008) Tropomyosin-based regulation of the actin cytoskeleton in time and space. *Physiol Rev* 88:1-35.

Gurtner GC, Werner S, Barrandon Y, Longaker MT (2008) Wound repair and regeneration. *Nature* 453:314-21.

Hook J, Lemckert F, Schevzov G, Fath T, Gunning P (2011) Functional identity of the gamma tropomyosin gene: Implications for embryonic development, reproduction and cell viability. *Bioarchitecture* 1:49-59.

Ishikawa R, Yamashiro S, Matsumura F (1989) Differential modulation of actin-severing activity of gelsolin by multiple isoforms of cultured rat cell tropomyosin. Potentiation of

protective ability of tropomyosins by 83-kDa nonmuscle caldesmon. *J Biol Chem* 264:7490-7.

Kapoor M, Liu S, Shi-wen X, Huh K, McCann M, Denton CP, *et al.* (2008) GSK-3beta in mouse fibroblasts controls wound healing and fibrosis through an endothelin-1-dependent mechanism. *J Clin Invest* 118:3279-90.

Kim JH, Cho A, Yin H, Schafer DA, Mouneimne G, Simpson KJ, *et al.* (2011) Psidin, a conserved protein that regulates protrusion dynamics and cell migration. *Genes Dev* 25:730-41.

Kiyokawa E, Hashimoto Y, Kobayashi S, Sugimura H, Kurata T, Matsuda M (1998) Activation of Rac1 by a Crk SH3-binding protein, DOCK180. *Genes Dev* 12:3331-6.

Kopecki Z, Cowin AJ (2008) Flightless I: an actin-remodelling protein and an important negative regulator of wound repair. *Int J Biochem Cell Biol* 40:1415-9.

Kopecki Z, Luchetti MM, Adams DH, Strudwick X, Mantamadiotis T, Stoppacciaro A, *et al.* (2007) Collagen loss and impaired wound healing is associated with c-Myb deficiency. *J Pathol* 211:351-61.

Lees JG, Bach CT, O'Neill GM (2011a) Interior decoration: Tropomyosin in actin dynamics and cell migration. *Cell Adh Migr* 5:181-6.

Lees JG, Bach CTT, Bradbury P, Paul A, Gunning PW, O'Neill GM (2011b) The actin-associating protein Tm5NM1 blocks mesenchymal motility without transition to amoeboid motility. *Oncogene* 30:1241-51.

Liu S, Kapoor M, Leask A (2009) Rac1 expression by fibroblasts is required for tissue repair in vivo. *Am J Pathol* 174:1847-56.

Margadant C, Frijns E, Wilhelmsen K, Sonnenberg A (2008) Regulation of hemidesmosome disassembly by growth factor receptors. *Curr Opin Cell Biol* 20:589-96.

Nobes CD, Hall A (1995) Rho, rac, and cdc42 GTPases regulate the assembly of multimolecular focal complexes associated with actin stress fibers, lamellipodia, and filopodia. *Cell* 81:53-62.

Nobes CD, Hall A (1999) Rho GTPases control polarity, protrusion, and adhesion during cell movement. *J Cell Biol* 144:1235-44.

Reynolds LE, Conti FJ, Lucas M, Grose R, Robinson S, Stone M, *et al.* (2005) Accelerated re-epithelialization in beta3-integrin-deficient- mice is associated with enhanced TGF-beta1 signaling. *Nat Med* 11:167-74.

Rich L, Whittaker P (2005) Collagen and Picrosirius Red staining: A polarized light assessment of fibrillar hue and spatial distribution. *Braz J Morphol Sci* 23:97-104.

Samuel MS, Lopez JI, McGhee EJ, Croft DR, Strachan D, Timpson P, *et al.* (2011) Actomyosin-mediated cellular tension drives increased tissue stiffness and beta-catenin activation to induce epidermal hyperplasia and tumor growth. *Cancer cell* 19:776-91.

Sanz-Moreno V, Gadea G, Ahn J, Paterson H, Marra P, Pinner S, *et al.* (2008) Rac activation and inactivation control plasticity of tumor cell movement. *Cell* 135:510-23.

Schevzov G, Fath T, Vrhovski B, Vlahovich N, Rajan S, Hook J, *et al.* (2008) Divergent regulation of the sarcomere and the cytoskeleton. *J Biol Chem* 283:275-83.

Schevzov G, Vrhovski B, Bryce NS, Elmir S, Qiu MR, O'Neill GM, *et al.* (2005) Tissue-specific tropomyosin isoform composition. *J Histochem Cytochem* 53:557-70.

Schevzov G, Whittaker SP, Fath T, Lin JJ, Gunning PW (2011) Tropomyosin isoforms and reagents. *Bioarchitecture* 1:135-64.

Singer AJ, Clark RA (1999) Cutaneous wound healing. *N Engl J Med* 341:738-46.

Tojkander S, Gateva G, Schevzov G, Hotulainen P, Naumanen P, Martin C, *et al.* (2011) A molecular pathway for myosin II recruitment to stress fibers. *Curr Biol* 21:539-50.

Tomasek JJ, Gabbiani G, Hinz B, Chaponnier C, Brown RA (2002) Myofibroblasts and mechano-regulation of connective tissue remodelling. *Nat Rev Mol Cell Biol* 3:349-63.

Tscharntke M, Pofahl R, Chrostek-Grashoff A, Smyth N, Niessen C, Niemann C, *et al.* (2007) Impaired epidermal wound healing in vivo upon inhibition or deletion of Rac1. *J Cell Sci* 120:1480-90.

Valles AM, Beuvin M, Boyer B (2004) Activation of Rac1 by paxillin-Crk-DOCK180 signaling complex is antagonized by Rap1 in migrating NBT-II cells. *J Biol Chem* 279:44490-6.

Vlahovich N, Kee AJ, Van der Poel C, Kettle E, Hernandez-Deviez D, Lucas C, *et al.* (2009) Cytoskeletal tropomyosin Tm5NM1 is required for normal excitation-contraction coupling in skeletal muscle. *Mol Biol Cell* 20:400-9.

Webb DJ, Brown CM, Horwitz AF (2003) Illuminating adhesion complexes in migrating cells: moving toward a bright future. *Curr Opin Cell Biol* 15:614-20.

Witke W, Sharpe AH, Hartwig JH, Azuma T, Stossel TP, Kwiatkowski DJ (1995) Hemostatic, inflammatory, and fibroblast responses are blunted in mice lacking gelsolin. *Cell* 81:41-51.

Wong JS, Iorns E, Rheault MN, Ward TM, Rashmi P, Weber U, *et al.* (2011) Rescue of tropomyosin deficiency in Drosophila and human cancer cells by synaptopodin reveals a role of tropomyosin alpha in RhoA stabilization. *EMBO J* 31:1028-40.

Zaidel-Bar R, Milo R, Kam Z, Geiger B (2007) A paxillin tyrosine phosphorylation switch regulates the assembly and form of cell-matrix adhesions. *J Cell Sci* 120:137-48.

Legends:

Figure 1: Cutaneous wound healing is accelerated at day 7 in γ9D -/- mice. (a) Expression of Tm5NM1/2 in skin using antibodies that recognize the γ9D exon. HSP70 probing is shown as loading control. (b) Haematoxylin and Eosin (H&E) stained transverse sections of full thickness wounds after 7 days (lines indicate the edges of wound area); scale bar = 500μm. Ep.-epidermis, Der.-dermis, Adi.-adipose tissue, Pan.-panniculus. (c) Histogram shows average wound length (μm), at the indicated time periods (n=12 wounds). (d) Digital images of wounds at the indicated time periods; scale bar = 1mm. (e) Average wound area (mm^2) and (f) average wound gape (mm), at the indicated time periods (n=12 wounds). *p<0.05, **p<0.01, N.S. = not significant.

Figure 2: Skin tissue organization, proliferation and contractility. (a) H&E, E-cadherin (magnification shown on the right) stained sections of epidermis; scale bars 20μm and 10μm (magnified images). (b) PSR staining; scale bar 50μm. (c) Collagen fibre type distribution. (d) PCNA stained nuclei in dermis (upper panels) and epidermis (lower panels); scale bar 40μm. Histograms show the percentage of PCNA positive nuclei. White arrowhead, non-proliferating cell; Black arrowhead, proliferating cell. Dotted lines indicate the basement membrane. (e) Collagen contraction assay. Bright field image in left panels; scale bar = 200μm; gels on the right; scale bar = 2mm. Histogram shows average gel area 3 days after release. Results are the average from triplicate independent experiments. N.S. = not significant. (f) Histogram shows average panniculus gape length (mm), at the indicated time periods (n>6 wounds).

Figure 3: Tm5NM1/2 expression in skin. (a) Western blot of Tm5NM1/2 in Tm5NM1/2 -/-, WT MEFs and skin keratinocytes and (b) quantification relative to HSP70. (c) Tm5NM1/2 expression during wound healing in WT mice. (d) Tm5NM1/2 expression, comparing levels at 3, 7 and 14 days after wounding to average levels in UW skin (n=3). (e) Tm5NM1 transgene expression: LC1 antibody recognizes the exogenous human protein. (f) Endogenous and exogenous Tm5NM1/2 expression: anti-γ9D antibodies bind both endogenous mouse and transgenic human proteins. (g) Average total Tm5NM1/2 expression (n=4) and (h) wound lengths in transgenic mice (n=10 wounds). (i) western blot and (j) densitometric quantification of Tm5NM1/2 expression during wound healing in transgenic mice (n=3). HSP70 shown to indicate loading. N.S. = not significant. *p<0.05

Figure 4: Tm5NM1 expression inversely correlates with paxillin phosphorylation and Rac activity. (a) Expression of paxillin (Pax) and phosphorylated paxillin (p-Pax) in unwounded (UW) mice (n=3). (b) Expression of Rac protein in WT and Tm5NM1/2 -/- MEF and B35 and B35.Tm5NM1 cells. (c) Rac GTPase pull-down assay. Immunoblots show positive (GTPγS) and negative (GDP) controls. Top panels show pull-downs from WT and Tm5NM1/2 -/- MEFs and bottom panels show pull-downs from B35 and B35.Tm5NM1 cells. All graphs show the average of three independent repeats and densitometry was performed using Image-J by comparing the ratio of gene of interest to housekeeping genes HSP70 or GAPDH. *p<0.05, ***p<0.001, N.S. = not significant.

Figure 5: Tm5NM1/2 regulation of lamellipodial protrusions. (a) Tm5NM1/2 -/- MEF expressing YFP-tagged Tm5NM1 scale, bar 20μm (i). The boxed region (i) is enlarged (ii), showing a montage of individual frames taken from time-lapse imaging of the YFP-Tm5NM1 transfected cell. Arrow heads point to extending lamellipodium. Arrows point to the appearance of new Tm5NM1-positive filaments. Images taken at 5 minute intervals. Scale bar 5μm**.** (b) Tm5NM1/2-/- MEFs transfected with expression vectors for YFP, YFP.Tm5NM1 and YFP.Tm5NM2, fixed and stained with paxillin antibodies to detect adhesions. Arrow points to paxillin-positive focal complexes along the edge of lamellipodia. Scale bar 20μm. (c) Percentage of the indicated transfected cell populations displaying focal complex-positive lamellipodia. Data are the average from three separate experiments, n>30 cells scored per transfection. ***$p<0.001$.

Supplementary Movie 1: Time-lapse movie of Tm5NM1/2 -/- mouse embryonic fibroblasts transfected with YFP.Tm5NM1. Cells were imaged with a 40x oil objective and images captured every 5 minutes for a total of 3 hours.

Figure 1

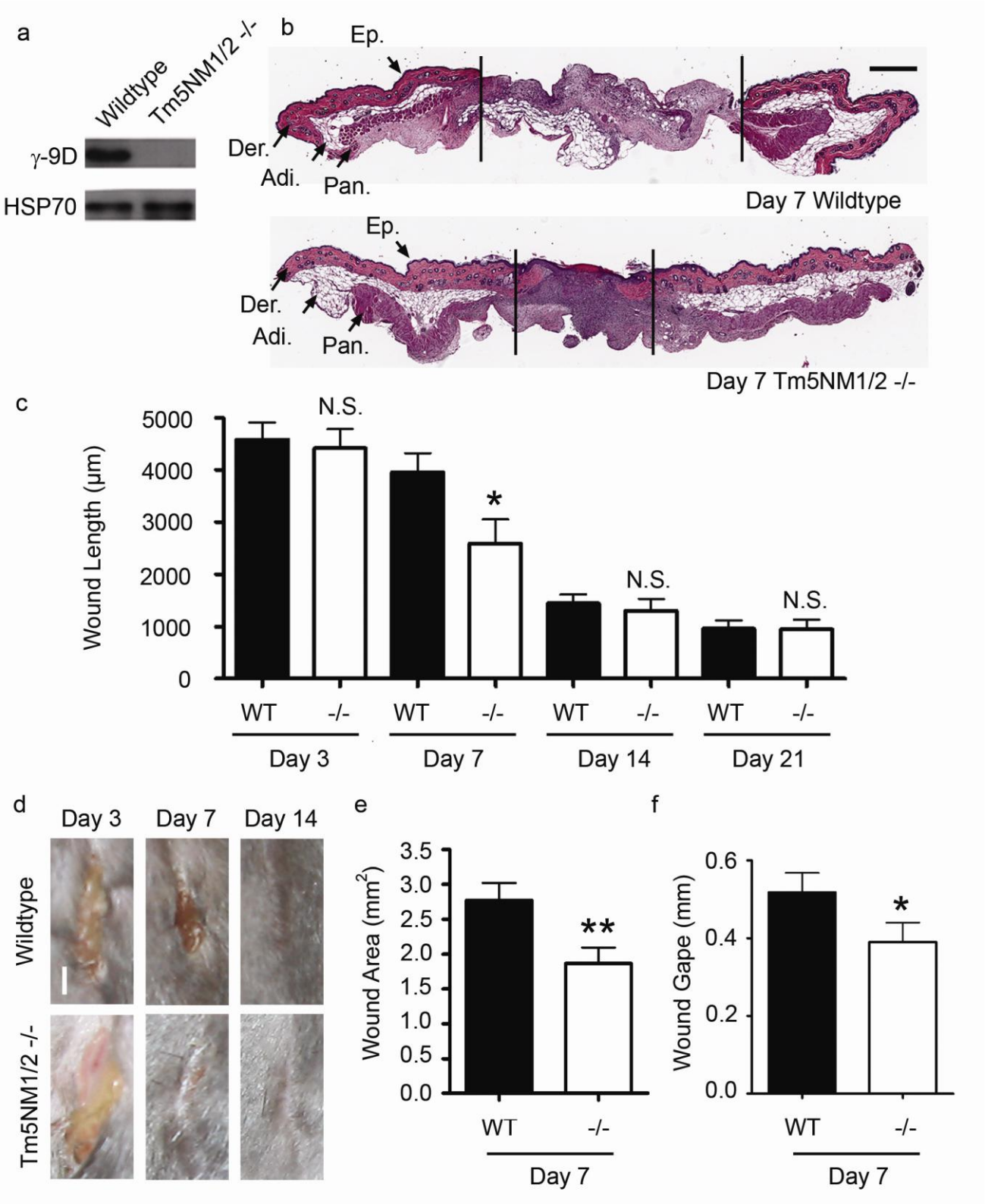
a
Wildtype
Tm5NM1/2 -/-
γ-9D
HSP70
b
Ep.
Der.
Adi.
Pan.
Day 7 Wildtype
Day 7 Tm5NM1/2 -/-
c
Wound Length (μm)
5000
4000
3000
2000
1000
0
N.S.
*
N.S.
N.S.
WT
-/-
Day 3
Day 7
Day 14
Day 21
d
Day 3
Day 7
Day 14
Wildtype
Tm5NM1/2 -/-
e
Wound Area (mm²)
3.5
3.0
2.5
2.0
1.5
1.0
0.5
0.0
**
WT
-/-
Day 7
f
Wound Gape (mm)
0.6
0.4
0.2
0.0
*
WT
-/-
Day 7

Figure 2

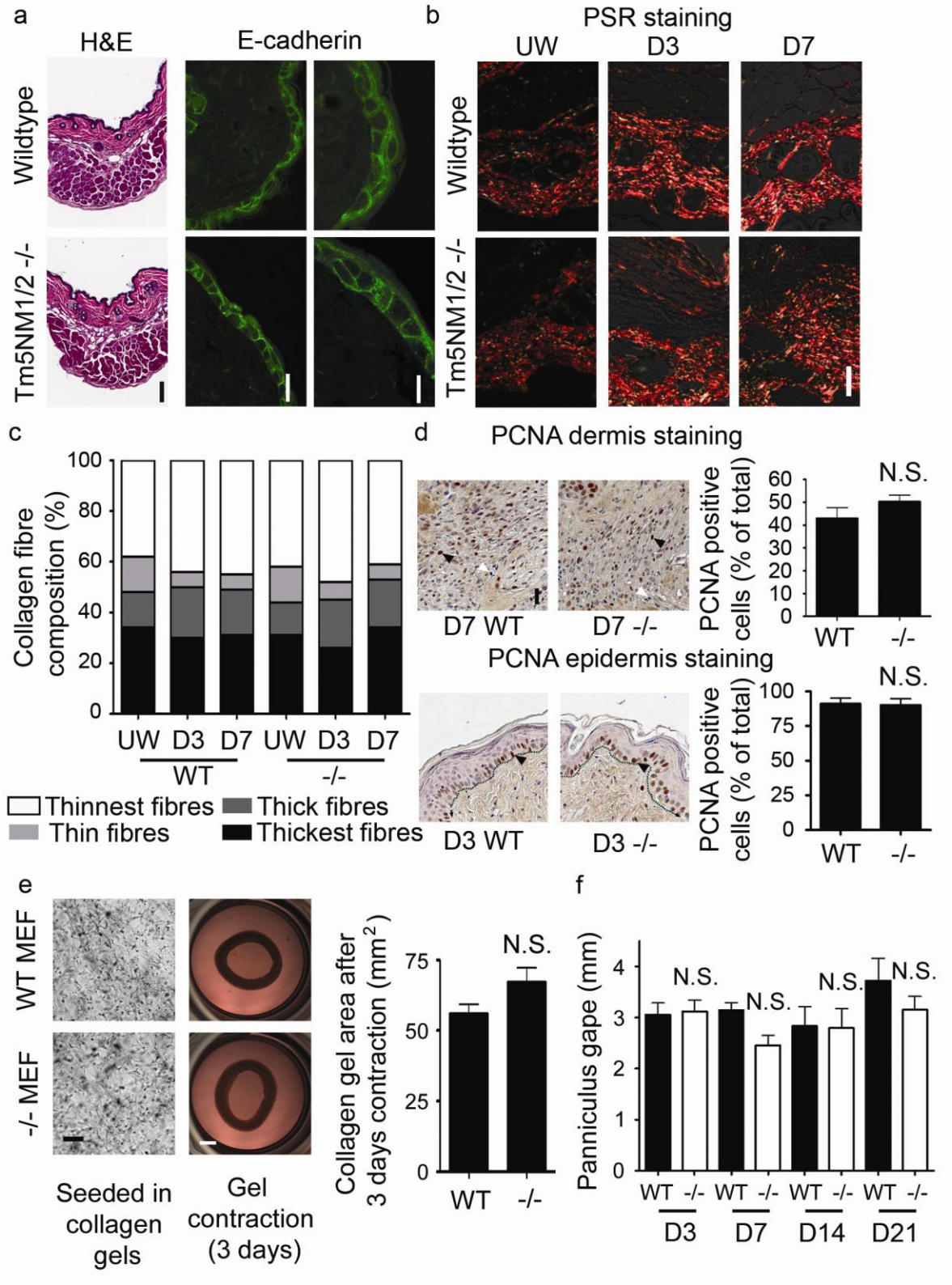
a
H&E
E-cadherin
Wildtype
Tm5NM1/2 -/-
b
PSR staining
UW
D3
D7
Wildtype
Tm5NM1/2 -/-
c
Collagen fibre composition (%)
100
80
60
40
20
0
UW D3 D7 UW D3 D7
WT
-/-
Thinnest fibres
Thick fibres
Thin fibres
Thickest fibres
d
PCNA dermis staining
D7 WT
D7 -/-
PCNA positive cells (% of total)
60
50
40
30
20
10
0
N.S.
WT
-/-
PCNA epidermis staining
D3 WT
D3 -/-
PCNA positive cells (% of total)
100
75
50
25
0
N.S.
WT
-/-
e
WT MEF
-/- MEF
Seeded in collagen gels
Gel contraction (3 days)
Collagen gel area after 3 days contraction (mm2)
75
50
25
0
N.S.
WT
-/-
f
Panniculus gape (mm)
4
3
2
1
0
N.S.
N.S.
N.S.
N.S.
WT -/- WT -/- WT -/- WT -/-
D3
D7
D14
D21

Figure 3

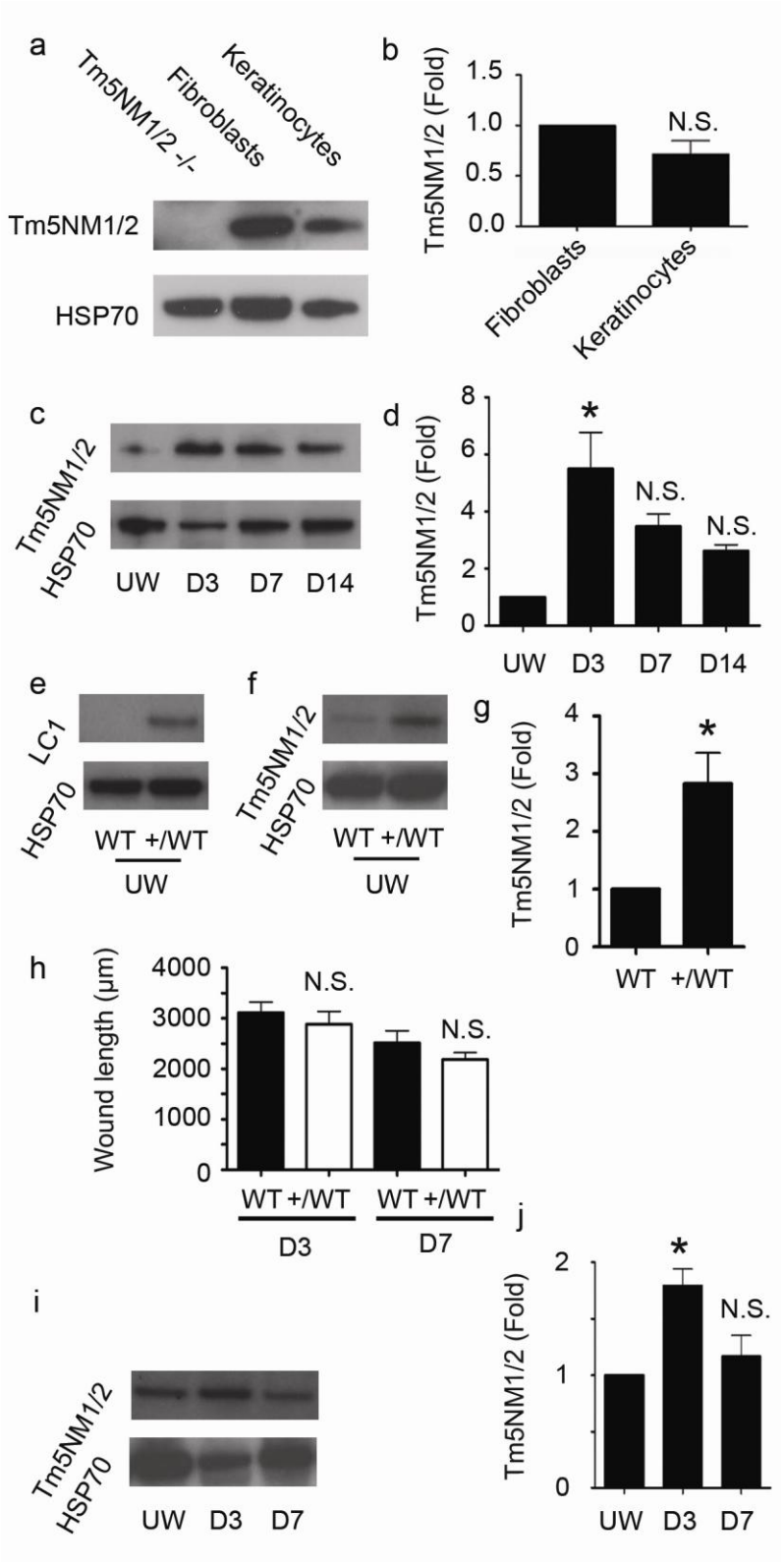
a
Tm5NM1/2 -/-
Fibroblasts
Keratinocytes
Tm5NM1/2
HSP70
b
Tm5NM1/2 (Fold)
1.5
1.0
0.5
0.0
N.S.
Fibroblasts
Keratinocytes
c
Tm5NM1/2
HSP70
UW D3 D7 D14
d
Tm5NM1/2 (Fold)
8
6
4
2
0
*
N.S.
N.S.
UW D3 D7 D14
e
LC1
HSP70
WT +/WT
UW
f
Tm5NM1/2
HSP70
WT +/WT
UW
g
Tm5NM1/2 (Fold)
4
3
2
1
0
*
WT +/WT
h
Wound length (μm)
4000
3000
2000
1000
0
N.S.
N.S.
WT +/WT WT +/WT
D3 D7
i
Tm5NM1/2
HSP70
UW D3 D7
j
Tm5NM1/2 (Fold)
2
1
0
*
N.S.
UW D3 D7

Figure 4

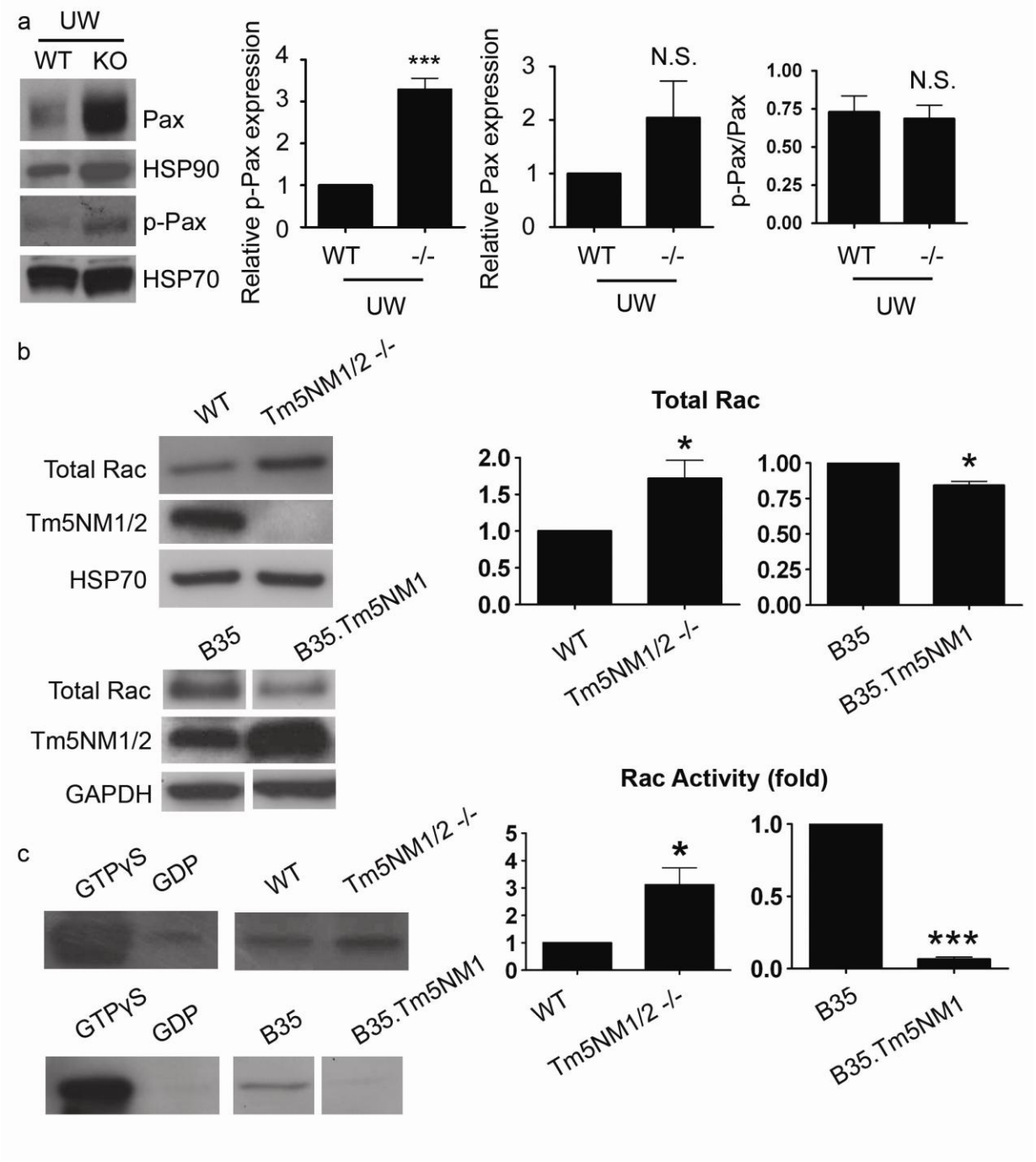
a
UW
WT KO
Pax
HSP90
p-Pax
HSP70
Relative p-Pax expression
***
WT -/-
UW
Relative Pax expression
N.S.
WT -/-
UW
p-Pax/Pax
N.S.
WT -/-
UW
b
WT Tm5NM1/2 -/-
Total Rac
Tm5NM1/2
HSP70
Total Rac
*
WT Tm5NM1/2 -/-
*
B35 B35.Tm5NM1
B35 B35.Tm5NM1
Total Rac
Tm5NM1/2
GAPDH
c
GTPγS GDP WT Tm5NM1/2 -/-
GTPγS GDP B35 B35.Tm5NM1
Rac Activity (fold)
*
WT Tm5NM1/2 -/-
***
B35 B35.Tm5NM1

Figure 5

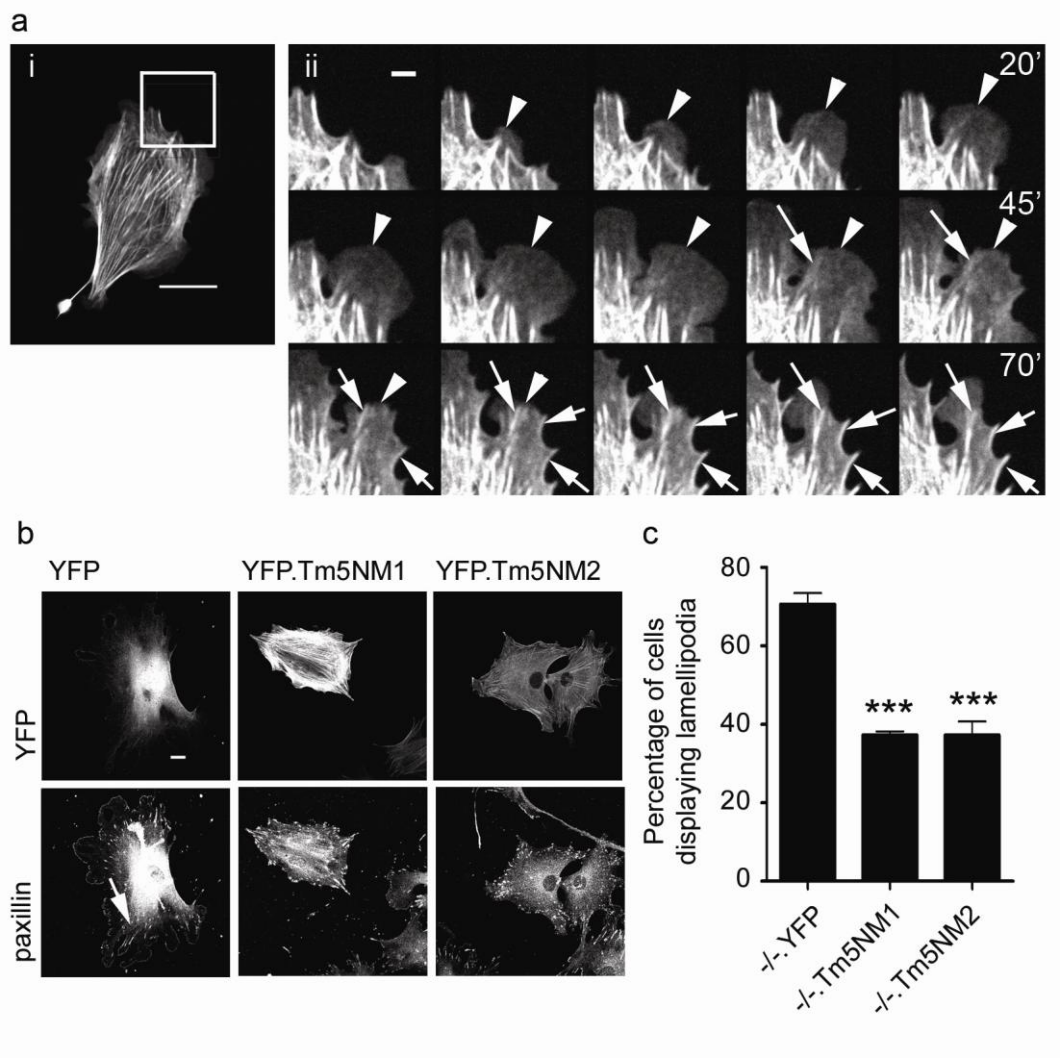
a
i
ii
20'
45'
70'
b
YFP
YFP.Tm5NM1
YFP.Tm5NM2
YFP
paxillin
c
Percentage of cells displaying lamellipodia
80
60
40
20
0
***
***
-/-.YFP
-/-.Tm5NM1
-/-.Tm5NM2